energy&fuels

Article

pubs.acs.org/EF

Gas Phase Mercury Oxidation by Halogens (Cl, Br, I) in Combustion Effluents: Influence of Operating Conditions

Itsaso Auzmendi-Murua and Joseph W. Bozzelli*

Department of Chemistry and Chemical Engineering, New Jersey Institute of Technology, Newark, New Jersey 07102, United States

ABSTRACT: Control of mercury emissions is one of the major challenges faced by power generation in coal burning and incineration plants, due to the increasing emission control regulations in the electricity generating sector. This study focuses on the elimination of mercury from the combustion flue gases via the oxidation of elemental mercury (nonsoluble) into its oxidized form (soluble) by the addition of halogens (chlorine, bromine, and iodine). A detailed reaction mechanism is developed and comparisons of mercury loss versus halogen, NO, SO_2, and H_2O presence in a typical combustion effluent stream are presented. The influence of different air-fuel equivalence ratios is also illustrated. The removal of mercury is evaluated with an elementary reaction mechanism (957 reactions, 203 species) developed from fundamental principles of thermodynamics and statistical mechanics. Thermochemistry and rate constants are from the literature or calculated at the M06-2X/aug-cc-pVTZ-PP (mercury species) and CBS-QB3 (nonmercury species) levels of theory. Rate constants are calculated by application of the Canonical Transition State Theory (CTST). Pressure dependence of chemically activated reactions is included by the QRRK analysis for k(E) and Master Equation for falloff. Thermochemistry on Hg halides, oxides, and Hg-NOx-X and Hg-SOx-X (X = Cl, Br) has been determined and kinetics incorporated in the mechanism. Results show that bromine and iodine are more effective than chlorine at oxidizing mercury due to competition for chlorine by hydrogen. Other results show that NO and SO_2 are observed to inhibit mercury conversion, that moderate changes in H_2O have a slight impact on mercury oxidation, and that the air-fuel ratio significantly influences the conversion of mercury by the halogens.

INTRODUCTION

The toxicity of mercury has been well-known for years, and the increase of its emissions to the atmosphere has become apparent in the last years. A study published by the CNR-Institute of Atmospheric Pollution Research determined that 2320 tons of mercury are emitted worldwide every year, from which 810 tons are from fossil-fuel fired plants, 400 tons from artisanal small scale gold mining, 310 tons from nonferrous metals manufacturing, 236 tons from cement production, 187 from waste disposal, and 163 tons from caustic soda production.[1] The increase of mercury emissions in Asia from coal burning and artisanal goal mining[2] since the 1950s is most significant.[2,3] The increasing concern on the toxicity of mercury has led many countries to implement regulations on the power generating and waste incineration plants for the control of mercury emissions. In January 2013, 140 nations adopted the first legally binding international treaty to set enforceable limits on emissions of mercury and exclude phase out or restrict some products that contain mercury, after four years of negotiations. In March 2015, the U.S. Environmental Protection Agency (EPA) interim final rule stated that the operator of electrical generating units should submit to EPA reports that include complete (not summary) mercury performance test data.[4]

Mercury is present in the combustion flue gases as elemental mercury (Hg^o), oxidized mercury (Hg^{2+}), and mercury associated with particles (Hg_p). Elementary mercury is highly volatile, and it is not feasible to capture it by using the usual air pollution control devices (scrubbers, electrostatic precipitators, fabric bags, ...). However, the oxidized mercury is water-soluble and has the tendency to associate to particles, and these forms can be eliminated by the air pollutant control devices. Figure 1 represents a schematic view of the usual control devices in a power generation plant. In the combustion chamber, mercury is present mainly as elemental mercury (Hg^o), with some oxidized mercury (Hg^{2+}) and mercury associated with particles (Hg_p). After the economizer, the selective catalytic reduction (SCR) or selective noncatalytic reduction (SNCR) systems aim to remove nitrogen oxides (NOx) from the combustion effluent, but they additionally succeed in oxidizing part of the elemental mercury into the oxidized Hg^{2+}, and part of the Hg^{2+} will also deposit in the particulate matter that is present. The goal of fabric filters (bag houses) or electrostatic precipitators (ESP) is the elimination of the particulate matter, and, therefore, part of the mercury that is associated with the particles is eliminated in this step. The flue-gas desulfurization (FGD) targets the removal of sulfur oxides (SOx) and additionally succeeds to remove most of the oxidized mercury that is still present in the system. However, only a small fraction of the elemental mercury is removed through the air pollutant control devices.

A number of power generating plants have started incorporating specific mercury removal technologies.[4,5] The most common technology is the injection of activated carbon, which promotes the attachment of mercury to the carbon particles. The injection of bromine to the flue gases has also been tested in power plants,[5] where bromine was proven to be effective at oxidizing mercury. The disadvantage of adding halogens is that they can cause corrosion problems, increase of halogen content in fly ash, and can increase the emissions of halogens from air pollution control devices (APCD),[6] and

Received: August 31, 2015
Revised: November 14, 2015

DOI: 10.1021/acs.energyfuels.5b01958
Energy Fuels XXXX, XXX, XXX−XXX

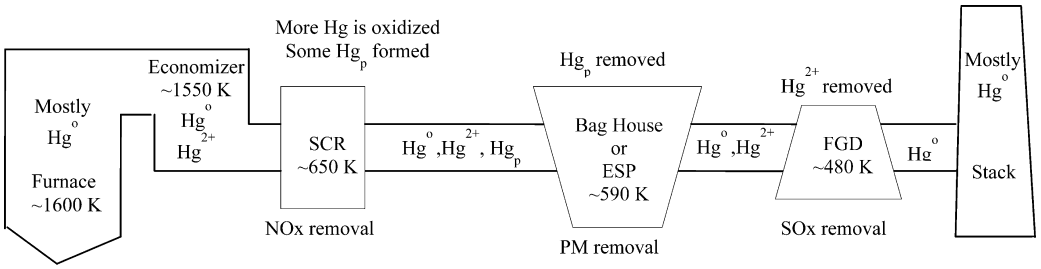

Figure 1. Schematic structure of air pollution control devices in a power generating plant.

therefore this must be accounted. Alternative techniques have been also proposed over the last years, such as mercury control by corona discharge,[7] circulating fluid bed for mercury and fine particulate control,[8] and electrocatalytic oxidation (ECO)[9] technologies. A recent publication written by an internationally acclaimed author team from government agencies, academia, and industry offers a detailed overview of the existing and currently researched technologies available for the control of mercury in coal-derived gas streams and that are viable for meeting the strict standards set by environmental protection agencies.[10] The approach followed in this work consists of the addition of halogens (chlorine, bromine, and iodine) to the combustion gases (added directly in the furnace), so that the elemental mercury (Hg^o) is converted into the oxidized mercury ($HgCl_2$, $HgBr_2$, HgI_2), and therefore removed by the air pollution control devices available in most power generating plants. A patent published in 2008 already describes the efficiency of adding bromine-containing compounds to the coal, or to the boiler combustion furnace, in order to enhance the oxidation of mercury.[11] The aim of this work is to develop an elementary reaction mechanism that described the reactions involved on the removal of mercury from the exhaust gases by the addition of halogens.

Different approaches have been presented for the elimination of NOx from combustion flue gases during the last years. One of the suggested solutions for the reduction of NOx emissions is oxi-combustion, where the combustion is performed with an oxidizer rich in O_2, instead of using air, reducing significantly the addition of N_2 in the system and therefore decreasing the concentration of NOx in the flue gases. There are, however, a few studies that have focused on determining the influence of the reduced NOx emissions in the conversion of mercury by the addition of halogens, and these are discussed just below. Technologies are also continuing on removal of sulfur from coal and natural gas in order to reduce the SOx emissions. It is therefore of value to determine the influence of the concentration of NOx and SOx in the speciation of mercury.

Our goal is to construct an elementary reaction mechanism to describe the oxidation of mercury by the addition of halogens in combustion effluents, as well as to determine the influence of the process conditions in the efficiency of oxidizing mercury.

The earliest mechanism for Hg^0 oxidation in a flue-gas stream was proposed by Hall et al.,[12] but it did not incorporate kinetic and thermochemical details. The formulation of a homogeneous, gas phase, mercury reaction mechanism started with a reaction scheme published by Widmer et al.[13,14] The mechanism consisted of an eight step elementary reaction sequence for the formation of $HgCl_2$ from Hg^0 and chlorine-containing species. Sliger et al.[15,16] studied the reactions of Hg^0 with HCl at various concentrations and temperatures and developed a model that incorporated a reaction set using H_2, O_2, CO, and CO_2 plus an additional reaction set of 18 equations involving Cl, Cl_2, HCl, ClO (chlorine monoxide), and HOCl. Senior et al.[17] included kinetic parameters for the homogeneous oxidation of elemental mercury by chlorine, using reactions from the literature. A later paper by Edwards et al.[18] extended the model proposed by Sliger et al.[15] by including more chlorination pathways, calculating new rate constants for some of the reactions, and including Hg reactions involving HgO. In addition to the eight-step reaction set, the authors added the following: (i.) a submechanism that described chlorine chemistry with nitrogen oxides (NOx) chemistry, (ii.) a moist CO oxidation submechanism, and (iii.) a H/N/O submechanism. The total mechanism included 102 elementary chemical reactions.

Xu et al.[19] listed, for the first time, the reactions along with the rate constants calculated from computational chemistry and transition state theory used in their model. Their mechanism included the Widmer et al.[13,14] Hg reactions, and they included 6 additional reactions containing HgO. Their work resulted in an oxidation model of 107 reactions and 30 species. Krishnakumar et al.[20] performed an evaluation of the available literature mechanisms, concluding that the Qiu mechanism predicted Hg oxidation in several experimental systems and conditions fairly accurately although it did not provide the best agreement in all cases. Zheng et al. have also investigated the kinetic mechanisms of reactions between mercury and oxidizing species by ab initio calculations of quantum chemistry.[21,22] Over the last years, the University of Utah has conducted several experimental studies on the oxidation of mercury by the addition of chlorine and bromine, as well as the influence of NOx and SOx on the conversion of mercury.[23−25] Ghorishi et al.[26] and Helble et al.[27] have also studied the influence of the sulfur oxides on the mercury oxidation. Peterson et al. have shown the HgO does not exist in the gas phase.[28]

Several groups have worked on the development of the thermochemical and kinetic properties of mercury reactions with chlorine,[29−34] bromine,[28,31,35−40] and iodine[37,41] at atmospheric and combustion conditions, that have been incorporated in the reaction mechanisms. We present and compare this data below.

The elementary reaction mechanism developed in this study (203 species and 957 reactions) is targeted to model and provide evaluation of conditions needed for conversion of elemental mercury into its oxidized form ($HgCl_2$, $HgBr_2$, HgI_2), trends in the chemistry of mercury in a coal combustion environment, and the influence of nitrogen oxides (NOx), sulfur oxides (SOx), the addition of vapor water (H_2O), the use of different temperature profiles, and the fuel/air equivalence ratio (CH_4 is the studied fuel) in the speciation of mercury.

DOI: 10.1021/acs.energyfuels.5b01958
Energy Fuels XXXX, XXX, XXX−XXX

COMPUTATIONAL METHODS

Development of Thermodynamic Properties. The thermochemical properties, heats of formation, entropies, and heat capacities (T) were determined from evaluation of literature values, and for new species, the thermochemical properties were calculated by use of computational chemistry with Density Functional Theory (DFT) based M06-2X/aug-cc-pVTZ-PP[42] (Augmented Correlation Consistent basis sets of Triple-ζ quality)[43,44] for mercury species and the DFT-based multilevel schemes G3,[45] CBS-QB3,[46] and CBS-APNO[47] for nonmercury species. All calculations were performed by the Gaussian 09 suite of programs[48] in conjunction with isodesmic work reactions for the determination of the enthalpies of formation.[49] Entropy and heat capacity contributions versus temperature are determined from the calculated structures, moments of inertia, nontorsion vibration frequencies, internal rotor parameters, symmetry, electron degeneracy, number of optical isomers, and the known mass of each molecule. The calculations use standard formulas from statistical mechanics for the contributions of translation, external rotation, and vibrations using the "SMCPS".[50]

Rate Constants. The rate constants were obtained from evaluation of literature values, and in the absence of actual rate data for the gas-phase reactions of mercury, Arrhenius constants ($k = AT^n \exp(-Ea/RT)$) were determined from the canonical transition state theory. Some kinetic parameters were estimated from similar reactions (generic reactions) and the known thermochemistry. Kinetics of small molecules in these system (several atoms species, example HgCl, $HgCl_2$, etc.) are in the low pressure or falloff kinetic regions with strong functions of temperature and pressure in the kinetics. Therefore, association, dissociation, and addition reactions were treated as chemical activation reactions with quantum Rice Ramsperger Kassel (qRRK) analysis for k(E) and master equation for falloff.[51,52]

Reaction Mechanism Development. The mechanism developed in this study has been divided into 8 submechanisms as described in Table 1. The mechanism incorporates elementary reaction kinetics and thermochemistry for the following: (1) mercury reaction with halogens (Cl, Br, I), hydroxides, nitrogen oxides (NOx), and sulfur oxides (SOx) with reactions taken from the literature[28,30−32,35−38,53] and developed during this study, (2) bromine reactions with hydroxides, nitrogen oxides (NOx), sulfur oxides (SOx), and C_1-C_2 hydrocarbons taken from the literature[54,55] and developed in this study, (3) chlorine reactions with hydroxides, nitrogen oxides (NOx), sulfur oxides (SOx), and C_1-C_2 hydrocarbons taken from the literature[54,56−61] and developed in this study, (4) iodine reactions with hydroxides, nitrogen oxides (NOx), and C_1-C_2 hydrocarbons hydrocarbons taken from the literature,[54] (5) chlorine-bromine-iodine reactions taken from the literature,[54] (6) hydroxide reactions (H_2, O_2) developed by Asatryan et al.,[62] (7) nitrogen oxidation reactions developed by Bozzelli et al.,[63] and (8) sulfur oxidation reactions developed by the University of Leeds.[64] Hydrocarbon reactions do not include molecular weight growth. The overall elementary reaction mechanism consists of 203 species and 957 reactions.

Solution (Numerical Integration) of the Elementary Kinetic Mechanism. The Chemkin Collection[65] was used to set up and solve the differential equations for a developed mechanism. Rate constants for the reverse reactions are determined from the thermochemistry and the forward rate constants (reactions are thermodynamically consistent). The AURORA Chemkin package was used for the simulation of the initial combustion of natural gas. Figure 2 represents a schematic view of the simulation model used for the combustion of natural gas and air in the combustion chamber. The PLUG Chemkin package was used to model the addition of the halogens in the furnace and the cooling process until the combustion effluent arrives to the exhaust. Figure 3 represents the schematic view of the model. Different temperature profiles were used.

RESULTS AND DISCUSSIONS

The initial concentrations and temperature profiles were taken from the experimental studies carried out in the University of

Table 1. Submechanisms, Number of Reactions, and Species Included in the Elementary Reaction Mechanism

	submechanism	no. of species	no. of reactions	refs
1	**Mercury-Halogen-Hydroxide-NOx-SOx**	48	96	
	mercury-bromine			32, 38[a]
	mercury-bromine hydroxide			35−37
	mercury-chlorine			32
	mercury-chlorine hydroxide			30, 31
	mercury-iodine			*a*
	mercury-chlorine-bromine-iodine			*a*
	mercury-hydroxide			*a*
	mercury-NO_x			*a*
	mercury-NO_x-halogen			*a*
	mercury-SO_x			*a*
	mercury-SO_x-halogen			*a*
2	**Bromine**	52	69	
	bromine-hydroxide			54, 72
	bromine-NO_x			54, 72
	bromine-SO_x			*a*
	bromo-methane oxidation			54, 72
3	**Chlorine**	59	234	
	chlorine-hydroxide			56−60, 73
	chlorine-NO_x			54, 72
	chlorine-SO_x			*a*
	chloro-methane oxidation			56−60, 73
4	**Iodine**	26	40	
	iodine-hydroxide			54, 72
	iodine-NO_x			54, 72
	iodine-methane oxidation			54, 72
5	**Halogens**	11	14	
	bromine−chlorine-iodine			54, 72
6	**H_2/O_2**	10	21	
				62
7	**Nitrogen Oxidation/NO**/NOx	74	372	
				63
8	**Sulfur Oxidation/SO**/SOx	23	111	
				64

[a]Developed this study.

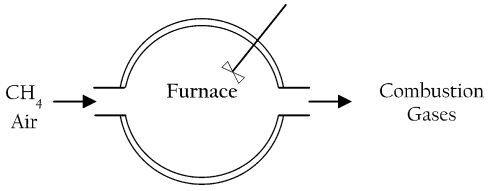

Figure 2. Schematic view of the simulation model for the combustion chamber.

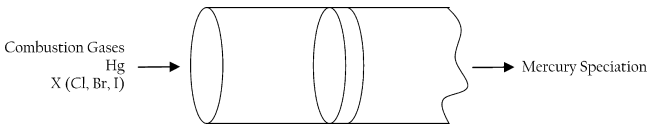

Figure 3. Schematic view of the simulation model for the addition of halogens and mercury in the furnace, plus the cooling process until the exhaust.

DOI: 10.1021/acs.energyfuels.5b01958
Energy Fuels XXXX, XXX, XXX−XXX

Table 2. Initial Concentration of the Natural Gas and Air Burned in the Combustion Chamber

species	concn (%)
CH_4	8
C_2H_6	0.4
C_3H_8	0.1
CO_2	0.1
O_2	19.2
N_2	72.2

Table 3. Initial Concentrations of the Combustion Effluent

species	concn
H_2	0.6%
O_2	1.9%
OH	0.6%
H_2O	16.5%
CO	1.4%
CO_2	7.8%
N_2	70.9%
NOx	0–60 ppmv
SOx	0–400 ppmv
Cl	0–500 ppmv
Br	0–40 ppmv
I	0–30 ppmv

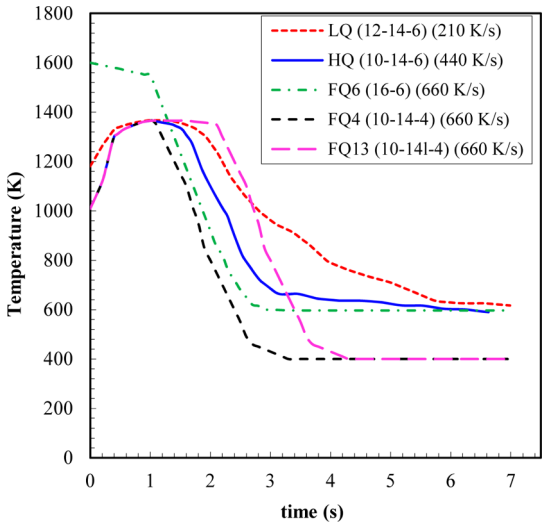

Figure 4. Temperature profiles used in Hg conversion mechanism runs.

Utah[23−25] for comparison of our modeling results with their experiment data. A natural-gas-fired combustor was used in their experiments. The initial natural gas and air concentrations used are summarized in Table 2. The initial concentrations and the concentration ranges used for the modeling of the combustion flue gases to study the oxidation of mercury are summarized in Table 3.

The conversion of mercury was determined as

$$\mathrm{Hg}\,(\%) = \frac{\mathrm{Hg_o} - \mathrm{Hg_f}}{\mathrm{Hg_o}} 100 \tag{1.1}$$

where $\mathrm{Hg_o}$ is the initial mole fraction of mercury in the combustion flue gases, and $\mathrm{Hg_f}$ is the final mole fraction of mercury in the combustion flue gases.

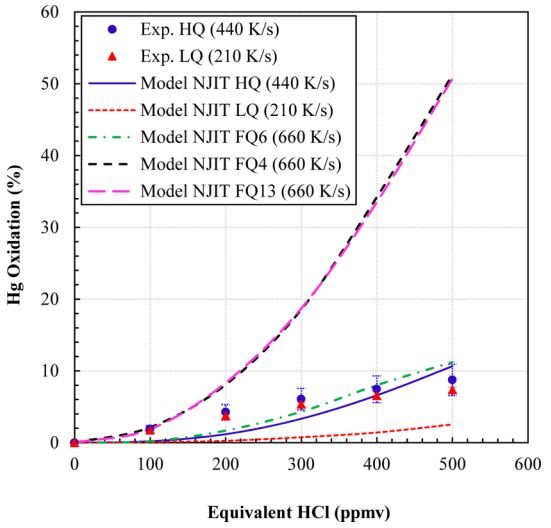

Figure 5. Mercury oxidation by the addition of chlorine.

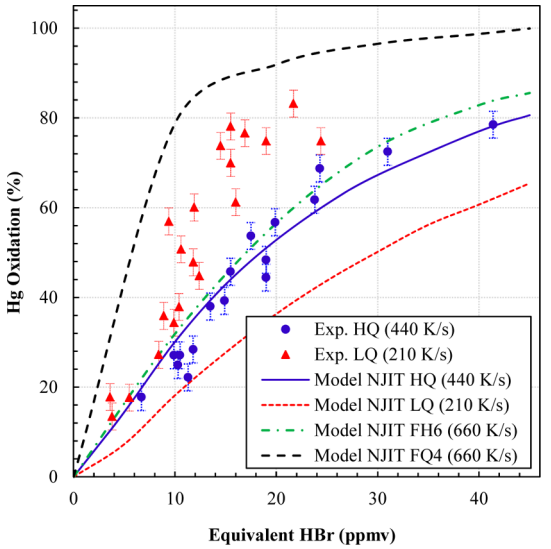

Figure 6. Mercury oxidation by the addition of bromine.

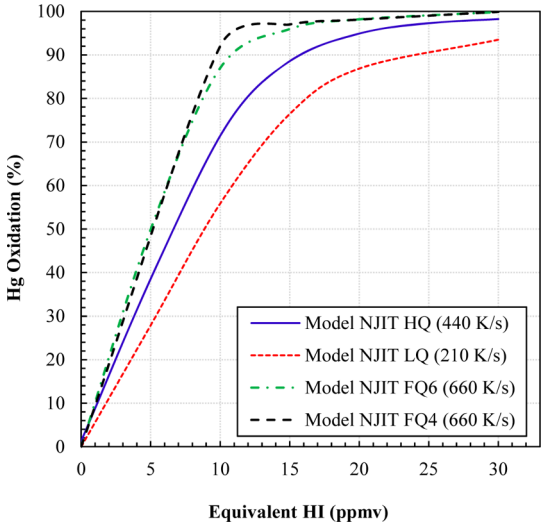

Figure 7. Calculated mercury oxidation by the addition of iodine.

DOI: 10.1021/acs.energyfuels.5b01958
Energy Fuels XXXX, XXX, XXX−XXX

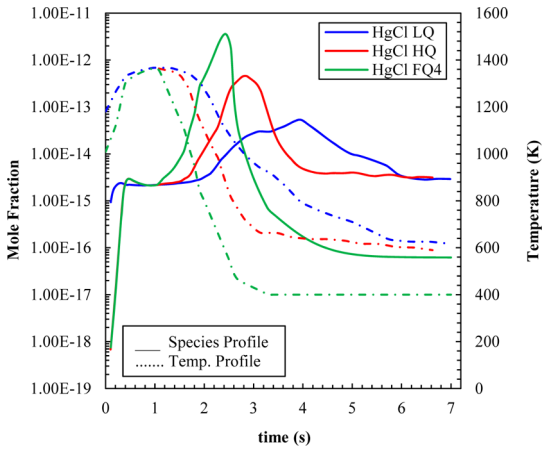

Figure 8. Mole fraction of HgCl versus time for initial NO of 30 ppm and Cl of 500 ppm for each of the temperature profiles.

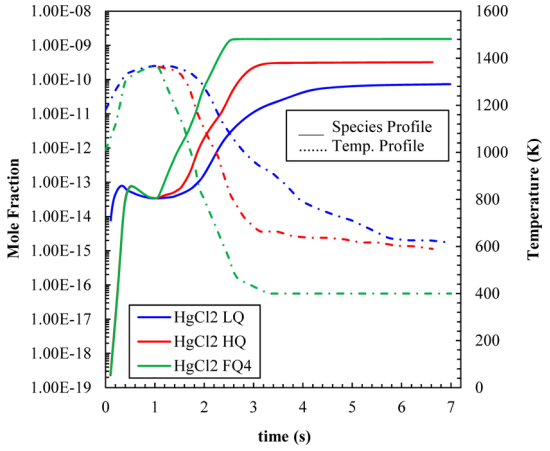

Figure 9. Mole fraction of HgCl versus time for initial NO of 30 ppm and Cl of 500 ppm for each of the temperature profiles.

Table 4. Enthalpies of Reaction of the Studied Hg/Cl, Hg/Br, andHg/I Reactions

	ΔH_{rxn} (kcal mol^{-1})		
reactions	Cl	Br	I
Hg + X ↔ HgX	−24.91	−13.53	−8.29
HgX + X_2 ↔ HgX_2 + X	−24.72	−25.95	−25.16
Hg + X_2 ↔ HgX + X	33.07	29.56	27.83
HgX + X ↔ HgX_2	−82.70	−72.04	−61.28
Hg + X_2 ↔ HgX_2	−49.63	−42.48	−33.45

The Utah Low Quench Temperature Profile, LQ (10-14-6), starts at 1181 K, achieves a maximum temperature of 1367 K, and has a slow cooling rate of 210 K per second to obtain the final temperature of 617 K. The Utah High Quench Temperature Profile, HQ (12-14-6), starts at a slightly lower temperature of 1009 K, increases the temperature until the maximum of 1366 K, and has a faster cooling rate of 440 K/s, until it obtains the final temperature of 590 K. The 1600−600 K Temperature Profile, FQ6 (16-6), starts at 1600 K and has a faster cooling rate, 660 K/s, to reach the final temperature of 600 K. The 1400−400 K Temperature Profile, FQ4 (10-14-4), starts at 1009 K, increases the temperature to a maximum of 1366 K, and, after remaining for ∼1 s at the maximum temperature, cools at 660 K/s, to a final temperature of 370 K.

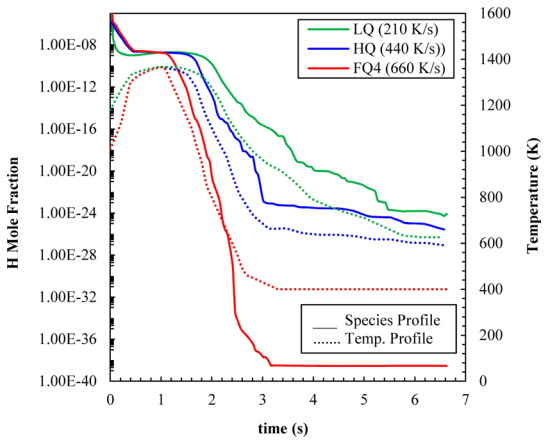

Figure 10. Mole fraction of hydrogen atom (H) versus time for initial NO of 30 ppm, and Cl of 500 ppm.

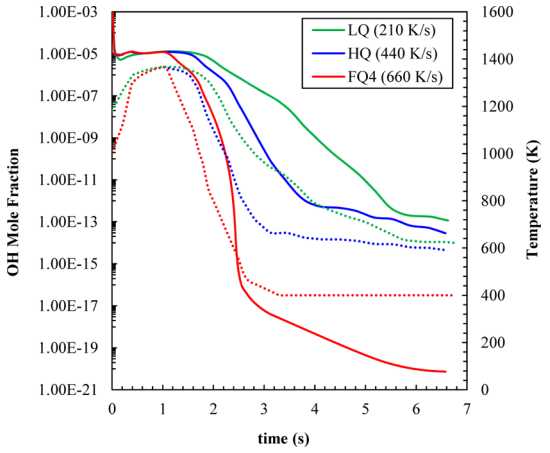

Figure 11. Mole fraction of hydroxide (OH) versus time for initial NO of 30 ppm and Cl of 500 ppm.

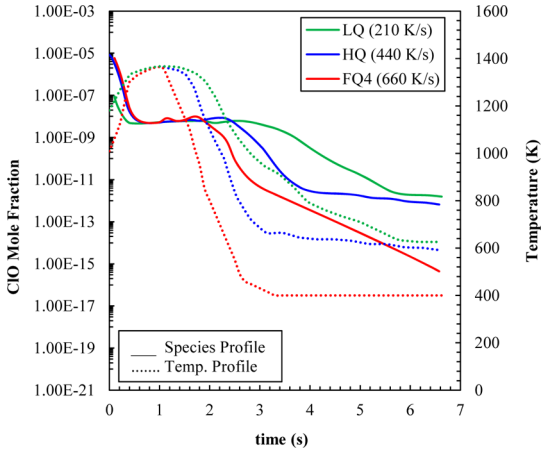

Figure 12. Mole fraction of ClO versus time for initial NO of 20 ppm and Cl of 500 ppm.

The 1400−400 K long Temperature Profile, FQ13 (10-14-4), starts at 1009 K, increases the temperature to a maximum of 1366 K, and, after remaining for ∼2 s at the maximum temperature, cools at 660 K/s, to a final temperature of 370 K. The temperature profiles are represented in Figure 4. f4

Influence of the Temperature Profiles and Halogens (Cl, Br, I). Simulations were carried out at the selected four

DOI: 10.1021/acs.energyfuels.5b01958
Energy Fuels XXXX, XXX, XXX−XXX

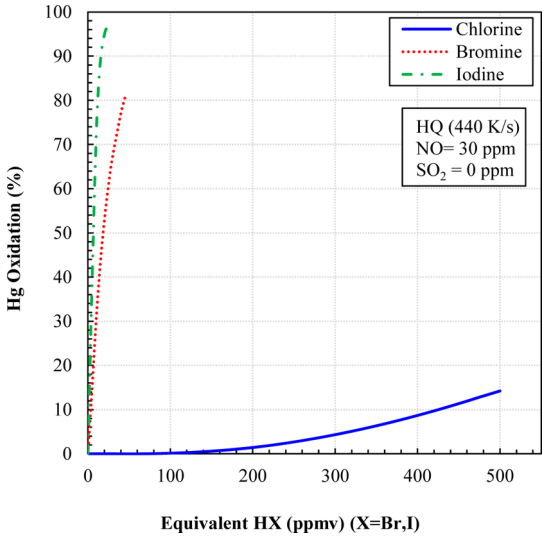

Figure 13. Mercury oxidation by the addition of chlorine, bromine, and iodine.

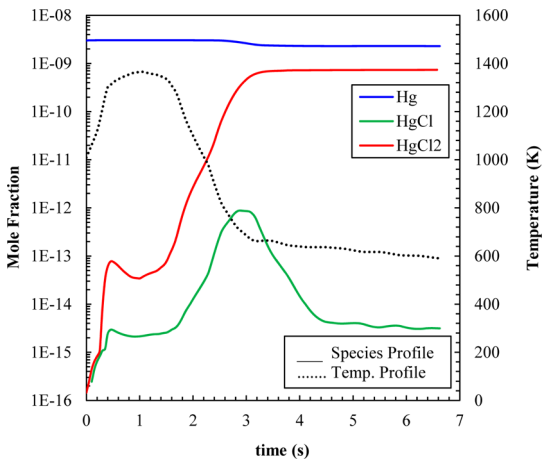

Figure 14. Mole fraction of Hg, HgCl, and $HgCl_2$ versus time for initial NO of 30 ppm and Cl of 500 ppm.

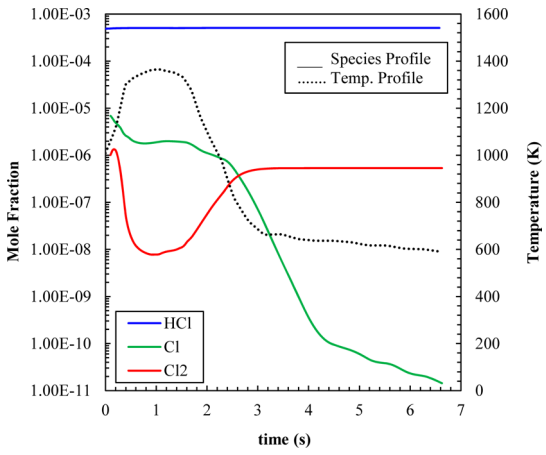

Figure 15. Mole fraction of HCl, Cl, and Cl_2 versus time for initial 30 ppm of NO and 500 ppm of Cl.

quench temperature profiles, in order to determine the influence of the temperature profile on the oxidation of mercury by chlorine, bromine, and iodine. The concentration of the halogens was varied, 0 to 500 ppm for chlorine (HCl), 0 to 40 ppm for bromine (HBr), and 0 to 30 ppm for iodine (HI), for each of the temperature profiles. Figures 5−7 illustrate the oxidation of mercury obtained when the halogens (chlorine, bromine, and iodine, respectively) are added to the system, for

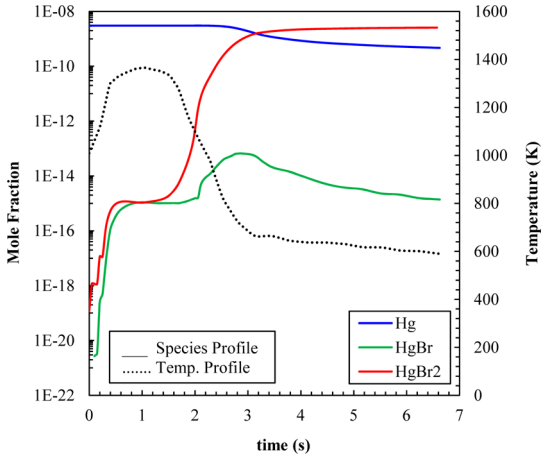

Figure 16. Mole fraction of Hg, HgBr, and $HgBr_2$ vs time for initial 30 ppm of NO and 40 ppm Br.

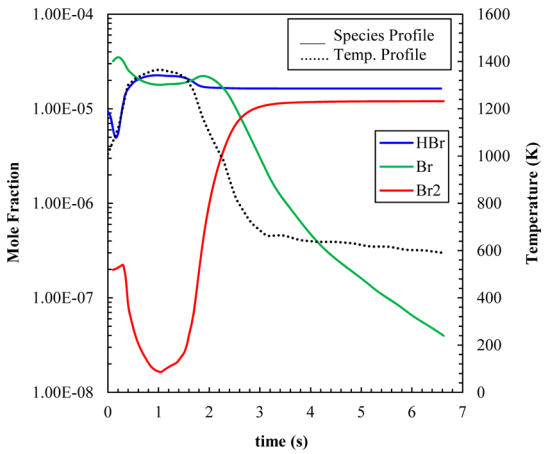

Figure 17. Mole fraction of HBr, Br, and Br_2 versus time for initial NO of 30 ppm and Br of 40 ppm.

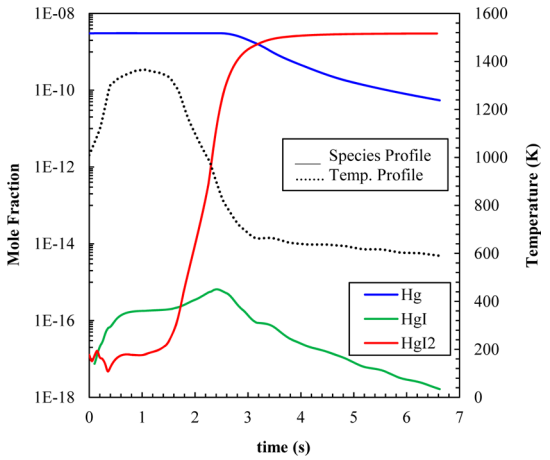

Figure 18. Mole fraction of Hg, HgI, and HgI_2 versus time for initial NO of 30 ppm and I of 30 ppm.

DOI: 10.1021/acs.energyfuels.5b01958
Energy Fuels XXXX, XXX, XXX−XXX

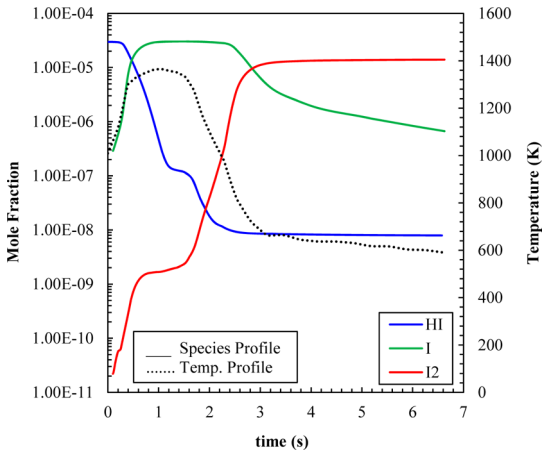

Figure 19. Mole fraction of HI, I, and I_2 versus time for initial NO of 30 ppm and of I 30 ppm.

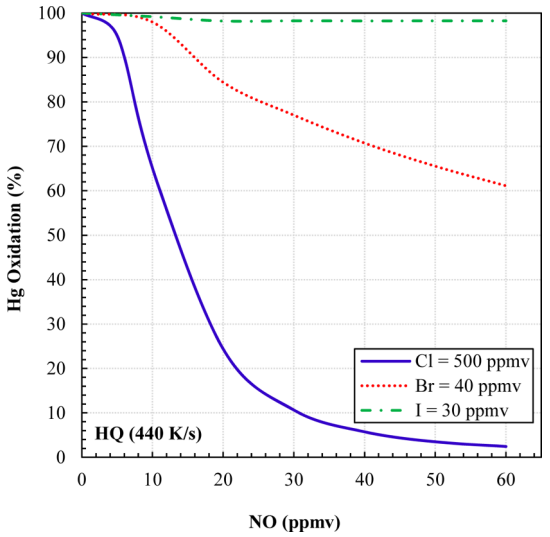

Figure 20. Influence of NO on the oxidation of mercury.

Table 5. Enthalpies of Reaction for Halogen NO Reactions[a]

reactions	ΔH_{rxn} Cl	Br	I
OH + XNO → HOX + NO	−18.1	−25.5	−31.3
H + X → HX	−103.1	−87.6	−71.3
X + NO → XNO	−38.4	−27.1	−20.3

[a]Units: kcal mol^{-1}.

each of the temperature profiles. The conversion is calculated as indicated in eq 1.1.

Results show that the higher temperature quench rate provides a higher conversion of the mercury compared to the lower temperature quench profile for all the halogens and that the temperature profile that has the fastest quench (660 K/s) and finishes at the lowest temperature (370 K) provides the highest conversion of mercury for all chlorine, bromine, and iodine addition. Calculation results indicate that the longer stay at the higher temperatures (temperature profile FQ13 compared to FQ4) does not result in a higher conversion of mercury. All temperature profiles have a high temperature region (1400−1600 K), which is necessary for the formation of the radical pool, so that mercury reacts with the atomic halogen (Hg + X → HgX). However, the higher quench temperature profile (FQ4 (660 K/s) has a longer residence time at the lower temperatures (370 K), which is necessary to keep some of the concentration of the unstable HgX species, so the HgX can further react to form the much more stable HgX_2. Figures 8 and 9 illustrate the concentration of HgCl and $HgCl_2$ versus time

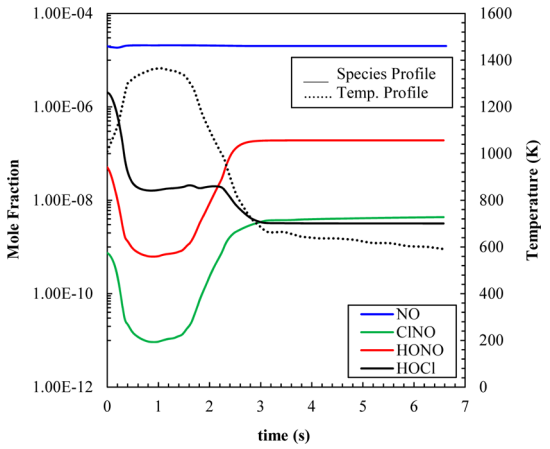

Figure 21. NO, ClNO, HONO, and HOCl mole fractions versus time for initial NO of 30 ppm and Cl of 500 ppm.

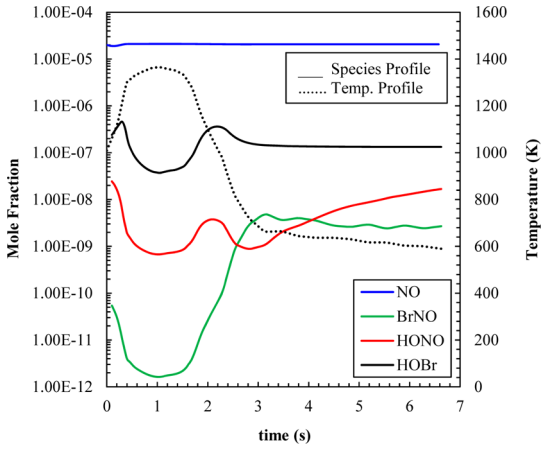

Figure 22. NO, BrNO, HONO, and HOBr mole fractions versus time for initial NO of 30 ppm and Br of 40 ppm.

Table 6. Catalytic Cycle of the Halogen-NOx Reactions[a]

reactions	ΔH_{rxn} Cl	Br	I	reactions	ΔH_{rxn} Cl	Br	I
X + NO → XNO	−38.4	−27.1	−20.3	X + NO → XNO	−38.4	−27.1	−20.3
X + XNO → X_2 + NO	−19.6	−19.0	−15.8	H + XNO → HX + NO	−64.7	−60.5	−51.0
X + X → X_2	**−58.0**	**−46.1**	**−36.1**	**H + X → HX**	**−103.1**	**−87.6**	**−71.3**

[a]Units: kcal mol^{-1}.

DOI: 10.1021/acs.energyfuels.5b01958
Energy Fuels XXXX, XXX, XXX−XXX

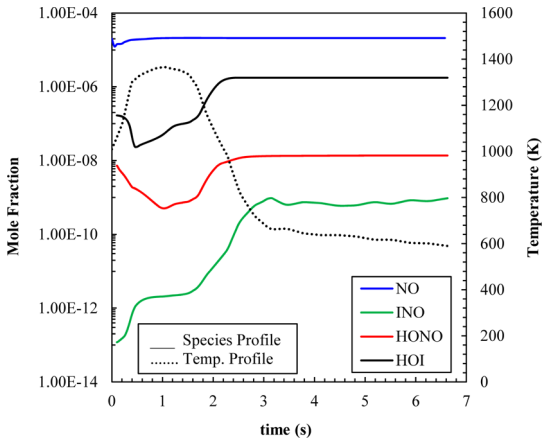

Figure 23. NO, INO, HONO, and HOI mole fractions versus time for initial NO of 30 ppm and I of 30 ppm.

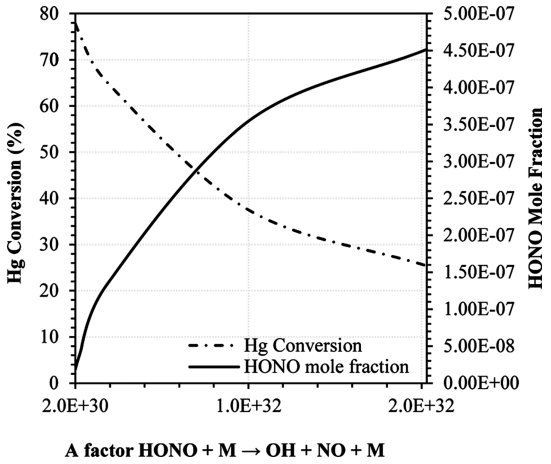

Figure 24. Sensitivity analysis of the HONO + M → OH + NO + M reaction.

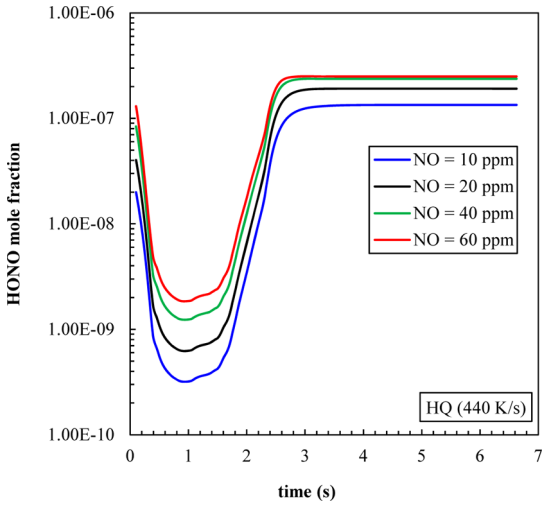

Figure 25. Concentration of HONO versus time for different initial NO concentrations.

for the different temperature profiles. The calculation results show that the formation of HgCl starts as soon as the system starts quenching, as well as the formation of $HgCl_2$. The conversion of mercury stops when the system achieves the stable low temperature

Table 4 summarizes the heats of reaction for the mercury halogen reactions discussed (the Hg——X bonds are very weak, 24.9, 13.5, and 8.3 kcal mol^{-1} for chlorine, bromine, and iodine respectively, whereas the XHg——X bonds are significantly stronger, 82.7, 72.0, and 61.3 kcal mol^{-1} for chlorine, bromine, and iodine, respectively).

Additionally, the species moles fraction profiles for hydrogen atom (H) and hydroxide (OH) (see Figures 10 and 11, respectively) show that the higher quench temperature profile leads to a decrease in their concentration, which means that less chlorine reacts with free hydrogen atoms, and there is more free chlorine is available to oxidize mercury. The profile of the mole fraction of ClO versus time (see Figure 12) shows that higher quench temperature profiles lead to the formation of lower concentrations of ClO, which results in having more free chlorine in the system to convert mercury into its oxidized form.

The results obtained in our simulations for chlorine and bromine were compared with the experimental results obtained by Van Otten et al.[25] in Figures 5 and 6 respectively. Results for chlorine (see Figure 5) show reasonable agreement for the high quench temperature profile, but the mercury conversion predicted by our mechanism for the lower temperature profile is lower than that obtained experimentally. Results for bromine (see Figure 6) show good agreement for the high quench temperature profile, but our modeling results predict that the lower quench temperature profile results in a lower conversion of mercury (as for chlorine), whereas their experimental results show that the lower quench temperature profile results in a higher conversion of mercury.

The concentration of HCl in the flue gas is usually on the order of 1−150 ppmv depending on the type of coal burned (bituminous or sub-bituminous). However, the concentration of iodine and bromine in the flue gases is much lower (0−3 ppm). Figure 13 shows a comparison between the conversion obtained by the addition of chlorine, bromine, and iodine for the high quench temperature profile. The results indicate that iodine and bromine are significantly more efficient for the conversion of mercury than chlorine. Significantly smaller concentrations of halogens would be needed to be added to convert mercury by the addition of bromine or iodine.

The Hg−Cl and ClHg−Cl bonds are stronger than the correspondent bonds for bromine and iodine (the Hg——X bonds 24.9, 13.5, and 8.3 kcal mol^{-1} for chlorine, bromine, and iodine, respectively, and the XHg——X bonds 82.7, 72.0, and 61.3 kcal mol^{-1} for chlorine, bromine, and iodine, respectively); however, results indicate that chlorine is much less effective when oxidizing mercury. Figures 14−19 show the profiles of the mole fraction of the mercury and halogen species versus time. Figures 14, 16, and 18 show that mercury is oxidized mainly to $HgCl_2$, $HgBr_2$, and HgI_2, which was expected, since these species are much more stable than HgCl, HgBr, and HgI.

Figure 15 shows that when chlorine is added to the system, the chlorine will be mainly present as HCl, because of its strong H−Cl bond (103.1 kcal mol^{-1}), which means that not much chlorine will be available to react with mercury. However, in the case of bromine, it is observed that HBr is not dominant (bond dissociation energy is 87.6 kcal mol^{-1}), which results in more bromine atoms being available to react with mercury (see Figures 16 and 17). For iodine, the decomposition of HI is significant (bond dissociation energy is 71.3 kcal mol^{-1}), which explains the efficiency of iodine when oxidizing mercury (see Figures 18 and 19).

DOI: 10.1021/acs.energyfuels.5b01958
Energy Fuels XXXX, XXX, XXX−XXX

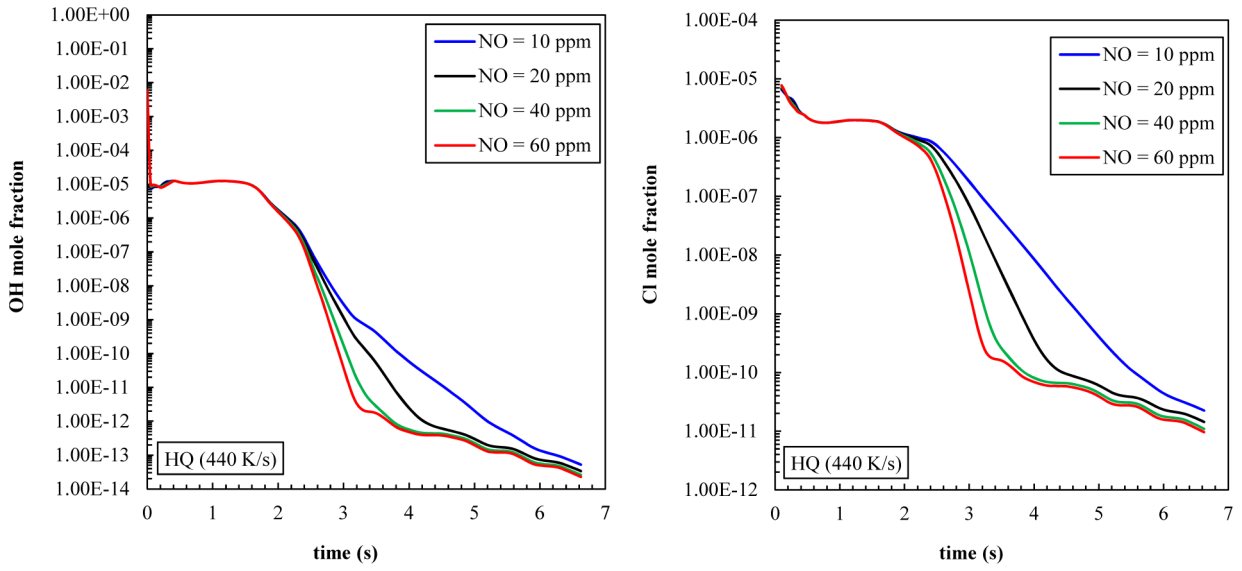

Figure 26. Concentration of OH and Cl versus time for different initial NO concentrations.

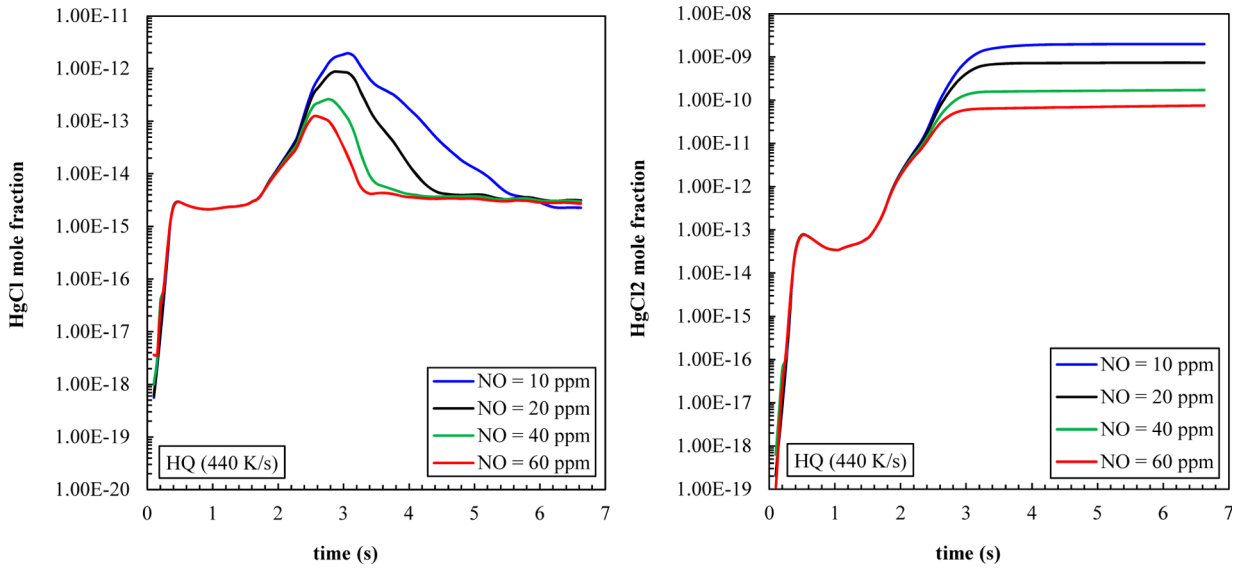

Figure 27. Concentration of HgCl and $HgCl_2$ versus time for different initial NO concentrations.

Influence of NOx. The influence of NOx on the oxidation of mercury by the addition of chlorine and bromine has been evaluated by several experimental and theoretical studies; however, several of these studies present opposing results. Laudal et al.[66] studied the oxidation of mercury in the presence of different concentrations and combinations of fly ash, NO/NO_2, SOx, HCl, and Cl_2. Their results showed that when no NOx was present in the system, the conversion was 84.8%, whereas in the presence of NOx the conversion of mercury dropped to 78.7%. Niksa et al.[67] predicted through their modeling results[68] that the lowest NO concentrations ([NO] < 20 ppm) enhance the conversion of mercury, whereas higher concentrations of NO inhibit homogeneous Hg oxidation, and they state that no oxidation of mercury is observed for NO concentrations above 100 ppm. Qiu and Helble[27] showed that NO inhibits mercury conversion, especially at lower concentrations of Cl_2. Byun et al. showed experimentally,[69] that when the NO concentration increased from 0 to 7 ppm in the presence of $NaClO_2$(s), the Hg oxidation increased significantly to give almost 100% of Hg oxidation, but that further increase of the NO concentration resulted in monotonic decrease of the Hg oxidation to about 60% at 180 ppm of NO. The presence of the $NaClO_2$ makes the analysis more complex. Van Otten et al.[25] concluded that increasing the NO concentration in the flue gas had no effect on Hg oxidation by chlorine or bromine, but their previous experimental study did report an inhibition effect of NO on the conversion of mercury.[70]

Figure 20 shows the modeling results obtained from this study. Results indicate that the presence of NO significantly decreases the oxidation of mercury by the addition of chlorine (Cl = 500 ppmv), decreases slightly the oxidation of mercury by the addition of bromine (Br = 40 ppmv), and does not have much effect when iodine (I = 30 ppmv) is added to the system.

Explanation for the inhibition of NO in the system includes formation of species such as X—NO where some are formed by reaction of HgX. For example, the reaction of HgX + NO → XNO + Hg is exothermic and decreases the HgX concentration. Analysis of X—Hg bond energies includes the

DOI: 10.1021/acs.energyfuels.5b01958
Energy Fuels XXXX, XXX, XXX−XXX

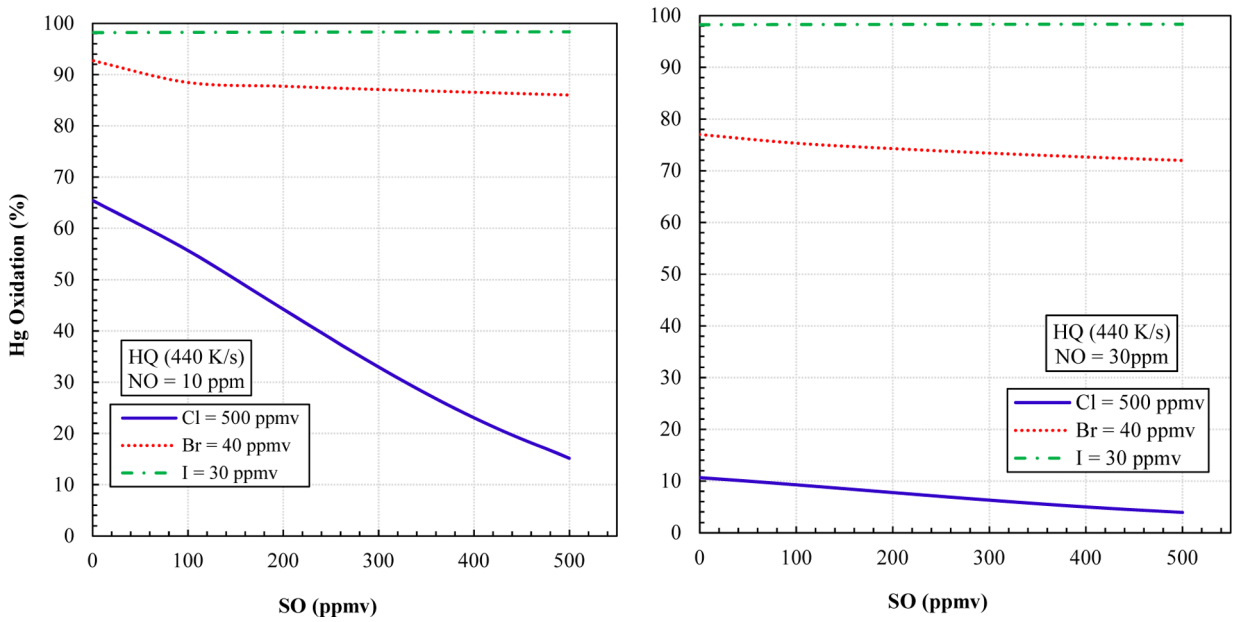

Figure 28. Influence of SO_2 on the oxidation of mercury for initial NO of 10 ppm (left) and NO of 30 ppm (right).

Table 7. Heats of Reaction for Halogen SO Reactions[a]

	ΔH_{rxn}		
reactions	Cl	Br	I
X + NO → XNO	−38.4	−27.1	−20.3
X + SO_2 → XSO_2	−15.5	−4.3	

[a]Units: kcal mol^{-1}

following: Cl−NO bonds are the strongest, followed by Br−NO and I−NO (see Table 5), in the presence of NO, several exothermic, catalytic cycles for loss of Cl to HCl (mainly) and Cl_2 can occur, inhibiting mercury oxidation, see Table 6. Once ClNO is formed, it can react with OH (ClNO + OH → HOCl + NO, ΔH_{rxn}= −18.1 kcal mol^{-1}), taking away OH from the system, which will inhibit mercury conversion.

Figures 21, 22, and 23 show the concentrations of NO, XNO, HONO, and HOX (X = Cl, Br, I), for the chlorine, bromine, and iodine systems, respectively. The species profiles in Figures 21−23 show the importance of the formation of HONO and HOX (X = Cl, Br, I) in all cases. However, because of the strong H−Cl bond, the influence of NO is stronger for the case when chlorine is added to the system. NO reacts with the OH produced by the radical pool (NO + OH → HONO, ΔH_{rxn} = 49.7 kcal mol^{-1}), taking away OH that reacts with H (H + OH → H_2O, ΔH_{rxn} = 118.8 kcal mol^{-1}) and therefore allowing there to be more free H that will react with Cl (Cl + H → HCl, ΔH_{rxn} = 103.1 kcal mol^{-1}), so that consequently chlorine will not be available to react with mercury. The sensitivity analysis of the reaction HONO + M → OH + NO + M indicates that the increase in the formation on HONO

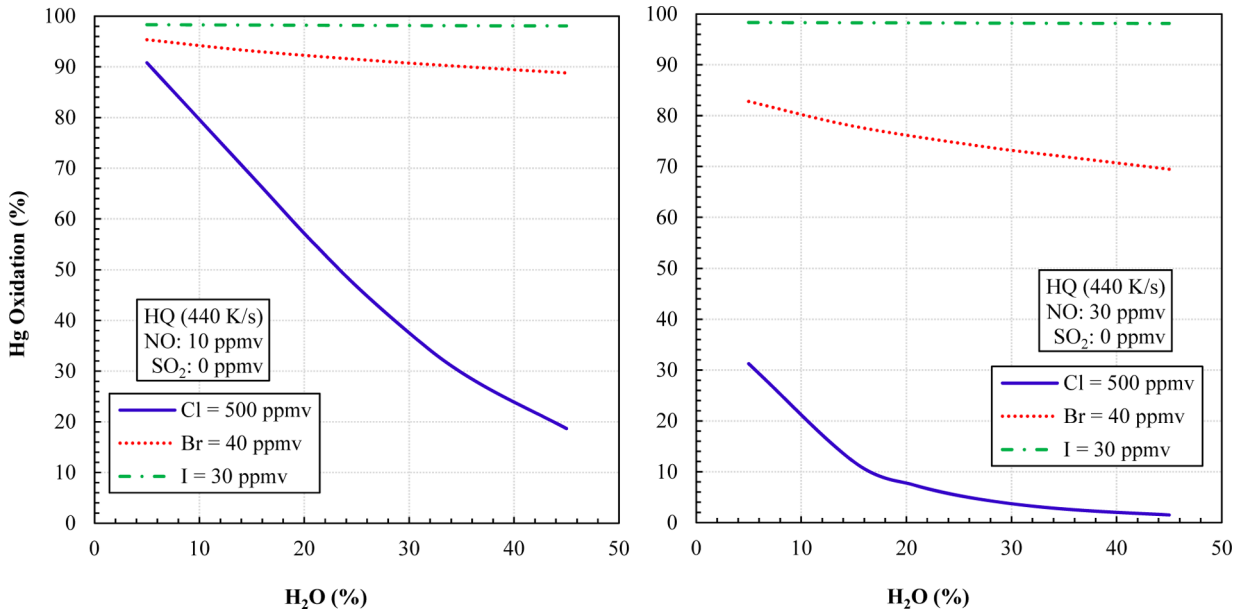

Figure 29. Influence of H_2O on the oxidation of mercury for initial NO of 10 ppm (left) and NO of 30 ppm (right).

DOI: 10.1021/acs.energyfuels.5b01958
Energy Fuels XXXX, XXX, XXX−XXX

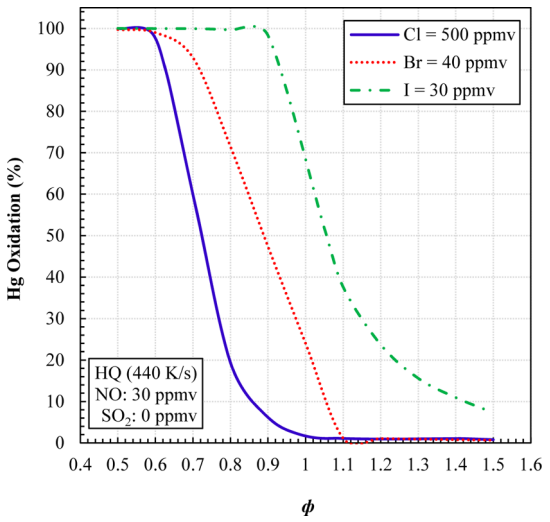

Figure 30. Influence of the equivalence ratio (ϕ) on the oxidation of mercury.

significantly reduces the conversion of mercury (see Figure 24). Figure 25 shows that the higher concentrations of NO lead to a higher formation of HONO, which results in a decrease in the concentration of OH in the reaction system (see Figure 26). The decrease of OH implies that more H atoms are available to react with Cl atoms, and, therefore, the concentration of Cl atoms also decreases (see Figure 26). The decrease in the concentration of Cl atoms causes the decrease of the formation of the intermediate HgCl and the decrease in the formation of the final product $HgCl_2$ (see Figure 27).

Influence of SOx. The effects of SO_2 on the conversion of mercury from the literature results are not well established. Ghorishi[26] showed that SO_2 can inhibit mercury oxidation with chlorine. Laudal et al.[66] showed that in the presence of SO_2, mercury conversion decreased from 84.8% to 1.9%, concluding that SO_2 has a significant inhibiting influence on mercury conversion. Additionally, Qiu and Helble[27] illustrated the decrease on the oxidation of mercury when increasing the concentration of SOx in the system. They studied the oxidation of mercury by the addition of 250 ppm of HCl with different concentrations of SO_2 (0, 100, 400, and 500 ppm) resulting on an oxidation of 67.7, 46.4, 29.7, and 21.9%, respectively, and by the addition of 500 ppm of HCl with different concentrations of SO_2 (0, 100, and 400 ppm) resulting in an oxidation of 94.5, 77.4, and 62.4%, respectively. In 2005, Lighty et al.[70] reported that when 300 ppm of SO_2 were added to the oxidation system, the mercury conversion dropped ~50%, for 500 ppm of HCl. However, in their work from 2011, Van Otten et al.[25] concluded that SO_2 did not have a significant effect on mercury oxidation by chlorine, except when the HCl concentration was greater than 400 ppmv. Smith et al.[71] observed inhibition or enhancement of mercury oxidation by chlorine when SO_2 was added to the system. They showed that when both HCl and SO_2 were present, mercury oxidation was enhanced in the presence of SO_2 when the concentration of HCl was 200 ppmv and inhibited in the presence of SO_2 when the concentration of HCl was 200 ppmv and inhibited when the concentration of HCl was 555 ppmv.

Results of our modeling calculations are illustrated in Figure 28, for two different NO concentrations (NO = 10 ppm, left, and NO = 30 ppm, right). SO_2 is much more stable (ΔH_f = −70.96 kcal mol^{-1}) than SO (ΔH_f = 1.20 kcal mol^{-1}), and consequently in combustion systems, sulfur is present mainly as SO_2. Therefore, in this work we have studied the influence of the addition of SO_2 in the combustion system. Results indicate that the presence of SO_2 decreases the oxidation of mercury by the addition of chlorine (Cl = 500 ppmv), specially at the lower concentrations of NO, and does not have much effect when bromine (Br = 40 ppmv) or iodine (I = 30 ppmv) are added to the system

SO_2 reacts mainly to form SO_3, so the reactions that affect the conversion of mercury mainly are $SO_2 + OH \rightarrow SO_3 + H$ and $SO_2 + O\ (+M) \rightarrow SO_3\ (+M)$. This explains why chlorine gets more affected by SO_2 than bromine and iodine. Additionally, X—SO_2 bonds are weaker than the X−NO bonds (see Table 7), which would explain why the influence of NOx is larger than the influence of SO_2 in the conversion of mercury.

Influence of H_2O. The aim is to study the influence of moisture in the conversion of mercury. Niksa et al. predicted in their simulations[68] that the addition of moisture to the system inhibited the oxidation of mercury (they observed the Hg oxidation fell from 100% to 54% when 8% of moisture was added to the system). Figure 29 summarizes the results obtained in this study for the effect of varying vapor water concentration (from 5 to 45%) on the oxidation of mercury, for two different concentrations of NO (10 and 30 ppm). Results show that the presence of water inhibits Hg oxidation. The conversion of mercury decreases from 31.2 to 1.5% when the concentration of water is increased for a concentration of NO of 30 ppm, and for a concentration of NO of 10 ppm, the conversion of mercury decreases more significantly, from 90.8 to 18.7%. As the concentration of H_2O increases, the main reason for this inhibition is the reaction $H_2O + Cl \rightarrow OH + HCl$ (ΔH_{rxn} = 15.5 kcal mol^{-1}), which removes Cl as HCl and consequently slows the conversion of mercury by chlorine. The influence on the conversion of mercury is smaller when bromine is added. The conversion of mercury decreases from 82.8 to 69.5% for initial NO of 30 ppm and from 95.3 to 88.8% for initial NO of 10 ppm. Calculation results show that the influence on the oxidation of mercury by addition of iodine is independent from the concentration of vapor water in the combustion system.

Influence of Fuel-Air Equivalence Ratio. The impact of the modification of the fuel to air equivalence ratio on the oxidation of mercury was studied. The fuel-air equivalence ratio is defined as indicated in eq 1.2

$$\phi = \frac{n_{fuel}/n_{oxidizer}}{(n_{fuel}/n_{oxidizer})_{stoichiometric}} \quad (1.2)$$

where n_{fuel} are the moles of the fuel, and $n_{oxidizer}$ are the moles of air (21% O_2 and 79% N_2). The fuel-rich mixture ($\phi > 1$) represents an excess of fuel, and the fuel-lean mixture ($\phi < 1$) represents an excess of oxidizer. The fuel used in this study is CH_4, which has the stoichiometric ratio ($n_{fuel}/n_{oxidizer}$) of 0.105. The results in Figure 30 show that fuel-lean mixtures ($\phi < 1$) lead to higher conversions of mercury for all chlorine, bromine, and iodine additions. For fuel-lean mixtures (excess of oxidizer) there is an excess of O_2 and the concentration of hydrogen is lower compared to fuel-rich mixtures. The presence of O_2 increases the oxidation of hydrocarbons and H_2 to H_2O and carbon to CO_2 and shifts the HCl concentration toward H_2O and Cl_2 allowing the halogen to oxidize Hg.

DOI: 10.1021/acs.energyfuels.5b01958
Energy Fuels XXXX, XXX, XXX−XXX

SUMMARY

An elementary reaction mechanism (957 reactions, 203 species) developed from fundamental principles of thermodynamics and statistical mechanics is evaluated for the study of the removal of mercury by the addition of halogens (chlorine, bromine, and iodine). Results illustrate that the use of high quench temperature profiles (660 K/s) that finish at lower temperatures (370 K) lead to an increase in the conversion of mercury, that iodine and bromine are more effective than chlorine (very small concentrations of iodine - 30 ppm - and bromine - 40 ppm - lead to >90% conversion of mercury), that NO, SO_2, and H_2O inhibit mercury conversion (significantly for the addition of chlorine and only slightly for the addition of bromine and iodine), and that the use of fuel-lean mixtures enhances the oxidation of mercury by chlorine, bromine, and iodine.

AUTHOR INFORMATION

Corresponding Author

*E-mail: Bozzelli@njit.edu.

Notes

The authors declare no competing financial interest.

ACKNOWLEDGMENTS

C. Senior and B. Van Otten of Reaction Enginerring International and A.R. Fry from the University of Utah are acknowledged for sharing the experimental data from the University of Utah. Dr. Rubik Asatryan is acknowledged for sharing his thermochemical calculations that have been added in the reaction mechanism. We thank the Basque Government for partial funding.

REFERENCES

(1) 2015, *November*.
(2) Streets, D. G.; Devane, M. K.; Bond, T. C.; Sunderland, E. M.; Jacob, D. J. *Environ. Sci. Technol.* **2011**, *45*, 10485−10491.
(3) Streets, D. G.; Zhang, Q.; Wu, Y. *Environ. Sci. Technol.* **2009**, *43*, 2983−2988.
(4) US Environmental Protection Agency (EPA) November 2015. http://www.epa.gov/hg/ (accessed Dec 1, 2015).
(5) Benson, S. A.; Holmes, M. J.; McCollar, D. P.; Mackenzie, J. M.; Crocker, C. R.; Kong, L.; Galbreath, K.; Dombrowski, K.; Richardson, C. *Final Report DOE NETL DE-FC26-03NT41991*; Energy and Environmental Research Center: Grand Forks, ND, 2007.
(6) Environmental Solutions, A. January 2013. http://www.adaes.com/ (accessed Dec 1, 2015).
(7) Helfritch, D. J.; Feldman, P. L. Coal Combustion Mercury Control by Means of Corona Discharge; IEEE International Conference on Plasma Science, 1999.
(8) Helfritch, D.; Feldman, P. L.; Pass, D. J. A Circulating Fluid Bed Fine Particulate and Mercury Control Concept; EPRI-DOE-EPA Combined Utility Air Pollutant Control Symposium, 1997.
(9) Powerspan, Clean Energy Technology 2013. http://powerspan.com/ (accessed Dec 1, 2015).
(10) Granite, E. J.; Pennline, H. W.; Senior, C. *Mercury Control: for Coal-Derived Gas Streams*; Wiley: Weinheim, Germany, 2014.
(11) Downs, W.; Farthing, G. A. Bromine Addition for the Improved Removal of Mercury from Flue Gas 2008; Vol. US 20080107579 A1.
(12) Hall, B.; Lindqvist, O.; Schager, P. *Water, Air, Soil Pollut.* **1991**, *56*, 3−14.
(13) Widmer, N. C. *Combust. Sci. Technol.* **1998**, *134*, 315−326.
(14) Widmer, N. C.; West, J.; Cole, J. A. Thermochemical Study of Mercury Oxidation in Utility Boiler Flue Gases; Proceedings of the Air & Waste Management Association 93rd Annual Conference and Exhibition, 2000, Salt Lake City, Utah.
(15) Sliger, R. N.; Kramlich, J. C.; Marinov, N. M. *Fuel Process. Technol.* **2000**, *65*−*66*, 423−438.
(16) Sliger, R. N.; Kramlich, J. C.; Marinov, N. M. Development of an Elementary Homogeneous Mercury Oxidation Mechanism; Proceedings of the Air & Waste Management Association 93rd Annual Conference and Exhibition, 2000, Salt Lake City, Utah.
(17) Senior, C. L.; Helble, J. J.; Mamani-Paco, R.; Sarofim, A. F.; Zeng, T. *Fuel Process. Technol.* **2000**, *63*, 197−213.
(18) Edwards, J. R.; Kilgroe, J. D.; Srivastava, R. K. *J. Air Waste Manage. Assoc.* **2001**, *51*, 869−877.
(19) Xu, M.; Qiao, Y.; Zheng, C.; Li, L.; Liu, J. *Combust. Flame* **2003**, *132*, 208−218.
(20) Krishnakumar, B.; Helble, J. J. *Environ. Sci. Technol.* **2007**, *41*, 7870−7875.
(21) Zheng, Z.; Liu, J.; Liu, Z.; Xu, M.; Liu, Y. *Fuel* **2005**, *84*, 1215−1220.
(22) Zheng, Z.; Liu, J.; Liu, Z.; Xu, M.; Liu, Y. *Fuel* **2007**, *86*, 2351−2359.
(23) Fry, A.; Lighty, J.; Senior, C.; Silcox, G. *Experimental and Kinetic Modeling Investigation of Gas-Phase Mercury Oxidation Reactions with Chlorine*, Ph.D. Dissertation, University of Utah, 2008.
(24) Fry, A. R.; Cauch, B.; Lighty, J. S.; Senior, C. L.; Silcox, G. D. *Proc. Combust. Inst.* **2007**, *31*, 2855−2861.
(25) Van Otten, B.; Buitrago, P. A.; Senior, C. L.; Silcox, G. D. *Energy Fuels* **2011**, *25*, 3530−3536.
(26) Ghorishi, S. B. *Fundamentals of Mercury Speciation and Control in Coal-Fired Boilers*; EPA-600/R-98-014; 1998.
(27) Qiu, J.; Helble, J. J.; Sterling, R. O. Development of an Improved Model for Determining the Effects of SO2 on Homogeneous Mercury Oxidation; Proceedings of the 28th International Technical Conference on Coal Utilization & Fuel Systems, March 10−13, 2003, Clearwater, FL.
(28) Shepler, B. C.; Peterson, K. A. *J. Phys. Chem. A* **2003**, *107*, 1783−1787.
(29) Liu, J.; Qu, W.; Yuan, J.; Wang, S.; Qiu, J.; Zheng, C. *Energy Fuels* **2010**, *24*, 117−122.
(30) Ariya, P. A.; Khalizov, A.; Gidas, A. *J. Phys. Chem. A* **2002**, *106*, 7310−7320.
(31) Khalizov, A. F.; Viswanathan, B.; Larregaray, P.; Ariya, P. A. *J. Phys. Chem. A* **2003**, *107*, 6360−6365.
(32) Wilcox, J. *J. Phys. Chem. A* **2009**, *113*, 6633−6639.
(33) Donohoue, D. L.; Bauer, D.; Hynes, A. J. *J. Phys. Chem. A* **2005**, *109*, 7732−7741.
(34) Yan, N. Q.; Liu, S. H.; Chang, S. G.; Miller, C. *Ind. Eng. Chem. Res.* **2005**, *44*, 5567−5574.
(35) Balabanov, N. B.; Peterson, K. A. *J. Phys. Chem. A* **2003**, *107*, 7465−7470.
(36) Balabanov, N. B.; Shepler, B. C.; Peterson, K. A. *J. Phys. Chem. A* **2005**, *109*, 8765−8773.
(37) Shepler, B. C.; Balabanov, N. B.; Peterson, K. A. *J. Phys. Chem. A* **2005**, *109*, 10363−10372.
(38) Wilcox, J.; Okano, T. *Energy Fuels* **2011**, *25*, 1348−1356.
(39) Donohoue, D. L.; Bauer, D.; Cossairt, B.; Hynes, A. J. *J. Phys. Chem. A* **2006**, *110*, 6623−6632.
(40) Liu, S. H.; Miller, C.; Yan, N. Q.; Liu, Z. R.; Qu, Z.; Wang, P. H.; Chang, S. G. *Environ. Sci. Technol.* **2007**, *41*, 1405−1412.
(41) Qu, Z.; Yan, N.; Liu, P.; Jia, J.; Yang, S. *J. Hazard. Mater.* **2010**, *183*, 132−137.
(42) Zhao, Y.; Truhlar, D. G. *Theor. Chem. Acc.* **2008**, *120*, 215−241.
(43) Peterson, K. A.; Figgen, D.; Goll, E.; Stoll, H.; Dolg, M. *J. Chem. Phys.* **2003**, *119*, 11113−11127.
(44) Peterson, K. A.; Puzzarini, C. *Theor. Chem. Acc.* **2005**, *114*, 283−296.
(45) Curtiss, L. A.; Raghavachari, K.; Redfern, P. C.; Rassolov, V.; Pople, J. A. *J. Chem. Phys.* **1998**, *109*, 7764−7776.
(46) Montgomery, J. A., Jr.; Frisch, M. J.; Ochterski, J. W.; Petersson, G. A. *J. Chem. Phys.* **1999**, *110*, 2822−2827.
(47) Ochterski, J. W.; Petersson, G. A.; Montgomery, J. A., Jr. *J. Chem. Phys.* **1996**, *104*, 2598−25619.

DOI: 10.1021/acs.energyfuels.5b01958
Energy Fuels XXXX, XXX, XXX−XXX

669 (48) Frisch, M. J.; Trucks, G. W.; Schlegel, H. B.; Scuseria, G. E.;
670 Robb, M. A.; Cheeseman, J. R.; Scalmani, G.; Barone, V.; Mennucci,
671 B.; Petersson, G. A.et al. *Gaussian 09, Revision A.1*; In Gaussian, Inc.:
672 Wallingford, CT, 2009.
673 (49) Asatryan, R.; Bozzelli, J. W.; Simmie, J. *J. Phys. Chem. A* **2008**,
674 *112*, 3172−3185.
675 (50) Sheng, C. Dissertation Thesis, 2002.
676 (51) Bozzelli, J. W.; Chang, A. Y.; Dean, A. M. *Int. J. Chem. Kinet.*
677 **1997**, *29*, 161−170.
678 (52) Chang, A. Y.; Dean, A. M.; Bozzelli, J. W. *Z. Phys. Chem.* **2000**,
679 *214*, 1533−1568.
680 (53) Goodsite, M. E.; Plane, J. M. C.; Skov, H. *Environ. Sci. Technol.*
681 **2004**, *38*, 1772−1776.
682 (54) IUPAC 2006 created by Nic, M.; Jirat, J.; Kosata, B. updates
683 compiled by A. D. Jenkins. http://goldbook.iupac.org (accessed Dec 1,
684 2015).
685 (55) Tsang, W.; Babushok, V. *Bromocarbon Mechanism NIST*
686 *(National Institute of Standards and Technology)*; 2001.
687 (56) Ho, W.; Barat, R. B.; Bozzelli, J. W. *Combust. Flame* **1992**, *88*,
688 265−295.
689 (57) Ho, W.; Bozzelli, J. W. *Twenty-Fourth Symposium on Combustion,*
690 *Combustion Inst.*, 1992, *Pittsburgh, PA*, 743−748.
691 (58) Ho, W.; Bozzelli, J. W. *Twenty-Fourth Symposium on Combustion,*
692 *Combustion Inst.*, 1992, *24*, 743−748.
693 (59) Ho, W.; Yu, C.; Bozzelli, J. W. *Combust. Sci. Technol.* **1992**, *85*,
694 23−63.
695 (60) Ho, W.; Yu, C.; Bozzelli, J. W. *Combust. Sci. Technol.* **1992**, *85*,
696 23−63.
697 (61) Tavakoli, J.; Chiang, H. M.; Bozzelli, J. W. *Combust. Sci. Technol.*
698 **1994**, *101*, 135−152.
699 (62) Asatryan, R.; Bozzelli, J. W.; Simmie, J. M. *Int. J. Chem. Kinet.*
700 **2007**, *39*, 378−398.
701 (63) Bozzelli, J. W.; Dean, A. M. Gas-Phase combustion Chemistry.
702 In *Combustion Chemistry of Nitrogen*; Springer, N., Ed.; W.C. Gardiner:
703 1999; Vol. Chapter 2.
704 (64) Hughes, K. J.; Tomlin, A. S.; Dupont, V. A.; Pourkashanian, M.
705 *Faraday Discuss.* **2001**, *119*, 337−352.
706 (65) Kee, R. J. *Senkin Manual. Chemkin Collection Release 3.6*; 2001.
707 (66) Laudal, D. L.; Brown, T. D.; Nott, B. R. *Fuel Process. Technol.*
708 **2000**, *65−66*, 157−165.
709 (67) Niksa, S.; Fujiwara, N. *J. Air Waste Manage. Assoc.* **2005**, *55*,
710 930−939.
711 (68) Niksa, S.; Helble, J. J.; Fujiwara, N. *Environ. Sci. Technol.* **2001**,
712 *35*, 3701−3706.
713 (69) Byun, Y.; Cho, M.; Namkung, W.; Lee, K.; Koh, D. J.; Shin, D.
714 N. *Environ. Sci. Technol.* **2010**, *44*, 1624−1629.
715 (70) Lighty, J. S.; Silcox, G.; Fry, A. *Fundamentals of Mercury*
716 *Oxidation in Flue Gas*; 2005.
717 (71) Smith, C.; Krishnakumar, B.; Helble, J. J. *Energy Fuels* **2011**, *25*,
718 4367−4376.
719 (72) *NIST-JANAF Themochemical Tables*, Fourth ed.; J. Phys. Chem.
720 Ref. Data, Monograph 9: Gaithersburg, MD, 1998.
721 (73) Tavakoli, J.; Chiang, H. M.; Bozzelli, J. W. *Combust. Sci. Technol.*
722 **1994**, *101*, 135−152.

DOI: 10.1021/acs.energyfuels.5b01958
Energy Fuels XXXX, XXX, XXX−XXX